Journal of Hazardous Materials 161 (2009) 423–430

Contents lists available at ScienceDirect

Journal of Hazardous Materials

journal homepage: www.elsevier.com/locate/jhazmat

Removal of fluoride from aqueous solution using protonated chitosan beads

Natrayasamy Viswanathan[a], C. Sairam Sundaram[b], S. Meenakshi[a,*]

[a] Department of Chemistry, Gandhigram Rural University, Gandhigram 624302, Tamilnadu, India
[b] Department of Science and Humanities, Karaikal Polytechnic College, Karaikal 609609, Puducherry, India

ARTICLE INFO

Article history:
Received 5 December 2007
Received in revised form 26 March 2008
Accepted 26 March 2008
Available online 1 April 2008

Keywords:
Protonated chitosan bead
Defluoridation
Adsorption
Freundlich
Langmuir

ABSTRACT

In the present study, chitosan in its more usable bead form has been chemically modified by simple protonation and employed as a most promising defluoridating medium. Protonated chitosan beads (PCB) showed a maximum defluoridation capacity (DC) of 1664 mg F^-/kg whereas raw chitosan beads (CB) possess only 52 mg F^-/kg. Sorption process was found to be independent of pH and altered in the presence of other co-existing anions. The sorbents were characterized using FTIR and SEM with EDAX analysis. The fluoride sorption on PCB follows both Freundlich and Langmuir isotherms. Thermodynamic parameters, viz., ΔG°, ΔH° ΔS° and E_a indicate that the nature of fluoride sorption is spontaneous and endothermic. The sorption process follows pseudo-second-order and intraparticle diffusion kinetic models. 0.1 M HCl was identified as the best eluent. The suitability of PCB has been tested with field samples collected from a nearby fluoride-endemic area.

1. Introduction

In recent times much public attention has been drawn to the fluoride content in drinking water and tooth paste. On the one hand, fluoride is added to drinking waters in small quantities to prevent dental caries. On the other hand, fluoride is a bone seeker and is linked to hip fractures and brittle bones [1]. Fluoride normally enters the environment and human body through water, food, industrial exposure, drugs, cosmetics, etc. However, drinking water is the single major source of daily intake [2]. The World Health Organization has specified the tolerance limit of fluoride content of drinking water as 1.5 mg/L [3]. The presence of a large amount of fluoride induces dental and skeletal fluorosis and non-skeletal fluorosis. The only option to prevent and control fluorosis is defluoridation of drinking water. Various methods have been suggested to reduce the fluoride concentration in drinking water, viz., adsorption [4,5], precipitation [6], ion-exchange [7], reverse osmosis [8], nano-filtration [9], electrodialysis [10] and Donnan dialysis [11]. Among the methods reported, adsorption is the most effective and widely used method for fluoride removal because of its ease of operation and cost effectiveness. The efficiency of adsorption technique depends upon the nature of adsorbents used. Many adsorbents were tried for fluoride removal namely activated alumina [4], hydrated cement [12], hydroxyapatite [13], activated carbon [14,15], quick lime [16], hydrotalcite [17], clay [18,19], ion exchanger [20], cotton cellulose [21], waste residue [22], geomaterials [23], plaster of Paris [24], brick powder [25], schwertmannite [26], composite [27], etc.

Since environmental protection is becoming an important global problem, biosorption has become a promising technique for removing toxic ions [28]. Chitosan is a linear polysaccharide of β-1, 4-*O*-glycosyl-linked glucosamine residue, derived from deacetylation of chitin which is a major component of crustacean shells and fungal biomass. Chitosan has increasingly been studied for the adsorption of different metal ions from dilute solution or wastewater [29,30]. Only a few reports are available about its capacity to remove anions [31–36]. In sorption process, chitosan is often used in the form of flakes or powder which is less stable and causes a significant pressure drop which would affect filtration during field applications. The defluoridation capacity (DC) of the unmodified chitosan was found to be minimum. These disadvantages outweigh its advantages of biodegradability, biocompatibility and indigenous. If chitosan has been modified into a form which could overcome the above mentioned challenges, then definitely it would throw more light on the field of defluoridation. Hence, in the present study, chitosan has been employed for the removal of fluoride from drinking water.

The present article, therefore, focuses on the development of cross-linked chitosan beads (CB) which is stable and can be regenerated and reused in subsequent operations and also avoid pressure drop during field applications. However, the enhanced DC could be achieved by protonation of cross-linked chitosan beads. The amino

* Corresponding author. Tel.: +91 451 2452371; fax: +91 451 2454466.
E-mail addresses: natrayasamy_viswanathan@rediffmail.com (N. Viswanathan), sairam_adithya@yahoo.com (C.S. Sundaram), drs_meena@rediffmail.com (S. Meenakshi).

0304-3894/$ – see front matter © 2008 Elsevier B.V. All rights reserved.
doi:10.1016/j.jhazmat.2008.03.115

group on each glucosamine residue within the chitosan chain can serve as a reactive site for chemical modifications. Hence, in order to effectively utilize the amine groups of chitosan for fluoride removal they have been modified into H^+ form (PCB), so that the DC of the chitosan could be significantly increased. This paper pertains to the systematic evaluation of the performance of the novel, chemically modified PCB for the uptake of fluoride. A comparative evaluation of the DC of chitosan beads with PCB was made. Suitability of PCB was tested under field conditions by collecting fluoride water in a nearby fluoride endemic area.

2. Experimental

2.1. Materials

Chitosan was supplied by Pelican Biotech and Chemicals Labs, Kerala (India). Its deacetylation degree is 85%. The viscosity of the chitosan solution was determined to be 700 (mPa s) by Brookfield Dial Reading Viscometer using electronic drive-RVT model (USA make). The chitosan solution was maintained at a constant viscosity for the beads preparation in order to maintain uniform molecular weight. NaF, NaOH, HCl, glacial acetic acid, glutaraldehyde and all other chemicals and reagents were of analytical grade. For the field study, water containing fluoride was collected from a nearby fluoride endemic village.

2.2. Preparation of cross-linked chitosan beads

Chitosan (20 g) was dissolved in 2.0% glacial acetic acid solution (1000 ml). The chitosan solution was dropped into a 0.5 M aqueous NaOH solution to form uniform chitosan beads. After gelling for a minimum 16 h in 0.5 M NaOH solution, the beads were washed with distilled water to a neutral pH. The wet beads were cross-linked with 2.5 wt% glutaraldehyde solution and the ratio of glutaraldehyde to chitosan beads was approximately 15 ml/g of wet beads. Cross-linking reaction occurred for 48 h and then cross-linked beads were washed with distilled water to remove any free glutaraldehyde.

2.3. Preparation of protonated cross-linked chitosan beads (PCB)

The PCB was prepared in order to effectively utilize the amino groups of cross-linked chitosan beads for fluoride sorption. The cross-linked chitosan beads were treated with concentrated HCl for 30 min for protonation of beads [32]. The PCB was washed with distilled water to neutral pH, dried at room temperature and used for sorption studies.

2.4. Sorption experiments

Sorption experiments were carried out by the batch equilibration method in duplicate. The sorbent used for this study was sieved to obtain uniform particle size of 0.6–1.2 mm. About 0.25 g of dry sorbent was added into 50 mL of 10 mg/L sodium fluoride solution with a desired pH value. The pH of the medium was adjusted with 0.1 M HCl or 0.1 M NaOH. The mixture was shaken in a shaker at a speed of 200 rpm at room temperature. Samples were taken at predetermined time intervals for the analysis of fluoride concentrations in the solutions until sorption equilibrium was reached. The DC of the sorbent was studied at different conditions including various dosages of sorbent, contact time of the sorbent for maximum defluoridation, pH of the medium, initial fluoride concentrations and the effect of competitor anions on defluoridation for optimization. The fluoride sorption on the sorbent was studied at different initial concentrations, viz., 11, 13, 15 and 17 mg/L of 50 ml solution and in the temperature range of 303, 313 and 323 K at neutral pH. The fluoride concentration was measured using an expandable ion analyzer EA 940 and the fluoride ion selective electrode BN 9609 (Orion, USA). The pH measurements were done with the same instrument with pH electrode. All other water quality parameters were analyzed using standard methods [37]. pH at zero point charge (pH_{zpc}) of beads was determined by pH drift method [38].

2.5. Characterization of sorbents

FTIR spectra of the chitosan samples were obtained using JASCO-460 plus model to confirm the presence of functional groups. Examination of beads with scanning electron microscope (SEM) with HITACHI-S-3000H model fitted with an energy dispersive X-ray analyzer (EDAX) allows a qualitative detection and localization of elements in the beads. The bead samples were coated with a thin layer of carbon in a vacuum coating unit. The SEM enables a direct observation of the surface microstructures of the chitosan beads and fluoride-sorbed beads. The specific surface area of the beads was analyzed using BET isotherm method with NOVA 1000 model.

Computations were made using Microcal Origin (Version 6.0) software. The goodness of fit and best model was discussed using regression correlation coefficient (r), coefficient of determination (r^2), chi-square and squared sum of errors (SSE) analysis.

3. Results and discussion

3.1. Instrumental analysis

The specific surface area of PCB was found to be 2.05 m^2/g. FTIR spectra are a useful tool to identify functional groups in a molecule, as each specific chemical bond often has a unique energy absorption band, and can obtain structural and bond information on a complex to study the strength and fraction of hydrogen bonding and miscibility [39]. FTIR spectrum of chitosan bead is shown in Fig. 1a. Although there is a possibility of overlapping between $-NH_2$ and –OH stretching vibrations, the strong broad band at the wavenumber region of 3300–3500 cm^{-1} is the characteristic of $-NH_2$ stretching vibration. The major bands for the chitosan bead can be assigned as follows: 3440 cm^{-1}(–OH and $-NH_2$ stretching vibrations), 2921 cm^{-1} (–CH stretching vibration in –CH and $-CH_2$), 1652 cm^{-1} ($-NH_2$ bending vibration), 1379 cm^{-1}(–CH symmetric bending vibrations in –CHOH–), 1067 and 1028 cm^{-1}(–CO stretching vibration in –COH) [39–41]. The FTIR spectrum of protonated cross-linked chitosan bead is presented in Fig. 1b. After cross-linking the chitosan beads, the –OH and $-NH_2$ stretching vibration around the wavenumber of 3440 cm^{-1} and the $-NH_2$

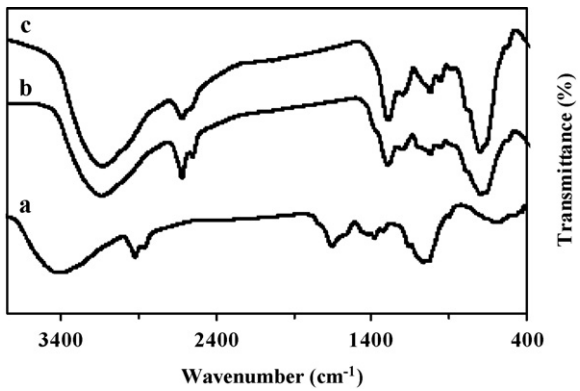

Fig. 1. FTIR spectra of (a) chitosan (b) PCB and (c) fluoride treated PCB.

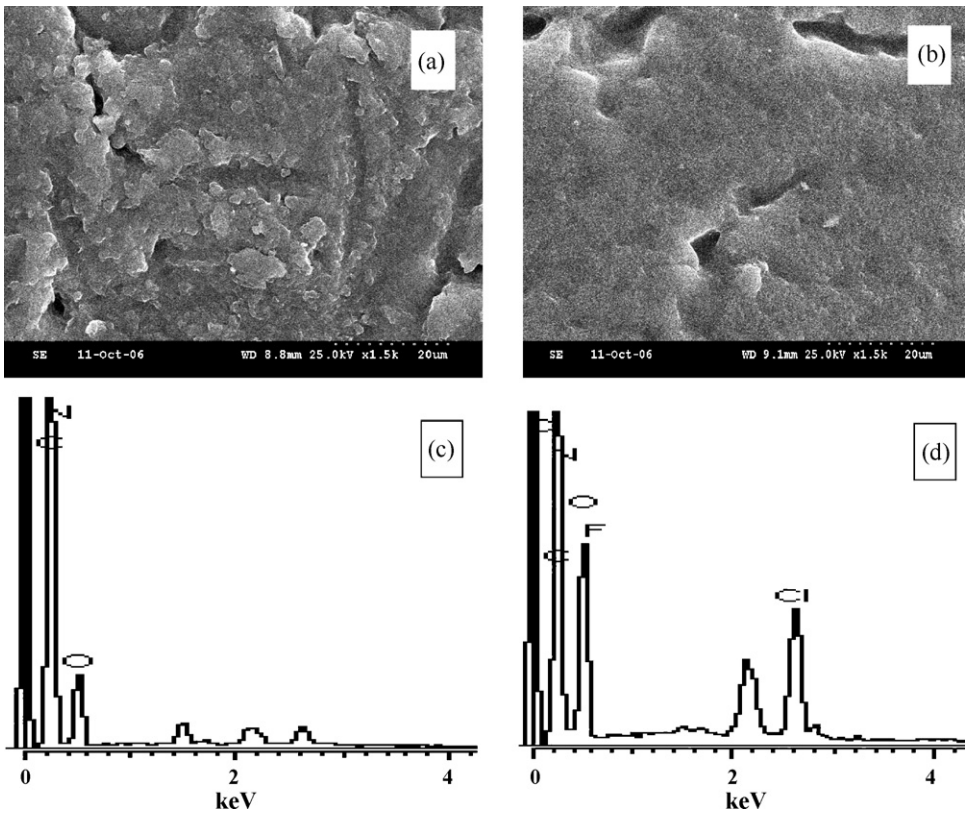

Fig. 2. SEM micrographs of (a) PCB and (b) fluoride-sorbed PCB, EDAX spectra of (c) PCB and (d) fluoride-sorbed PCB.

bending vibration at the wavenumber 1652 cm^{-1} were shifted to lower frequencies. The hydrogen bonding in amines is weaker than that of hydroxyl groups, so $–NH_2$ stretching bands are not as broad or intense as –OH stretching bands [42]. A slight broadening of $–NH_2$ stretching band in the fluoride sorbed PCB (Fig. 1c) may be taken as an indicative of hydrogen bonding between the protonated amine ($–NH_3^+$) and fluoride [42]. Similar results were reported by the authors while studying fluoride sorption onto chelating ion-exchange resins [5].

SEM was used to examine the structure of the sorbent. Fig. 2a and b show the SEM micrographs of PCB before and after fluoride sorption. There were apparent differences between the beads with many cavities before sorption and no such cavities are observed after sorption, it indicated fluoride sorption on PCB. The EDAX spectrum of PCB is given in Fig. 2c shows the presence of elements in it. An emergence of fluoride peak in the EDAX spectra of fluoride-treated PCB confirmed the fluoride sorption onto PCB which is shown in Fig. 2d.

The surface morphological changes of the chitosan beads were also confirmed by the shifting of pH_{zpc} values [43]. The pH_{zpc} of CB is 7.88 whereas for PCB this value shifted to 3.75. This clearly indicated the occurrence of structural changes in PCB.

3.2. Effect of contact time

Fig. 3a shows the variation of DC of the sorbents with respect to time and also the comparative difference between the unmodified and modified chitosan beads. Evidently, PCB has higher sorption ability for the uptake of fluoride than the raw CB. With respect to contact time, both the materials reached saturation after 30 min and for further experiments, 30 min was fixed as the period of contact for sorption studies. The PCB possesses the DC of 1664 mg F^-/kg whereas CB has only 52 mg F^-/kg. This clearly indicates that the protonated amine groups of PCB are responsible for higher DC than the original $–NH_2$ groups of chitosan bead. Since PCB has higher DC than chitosan bead, further discussions were limited only to PCB in order to explore the possibility of utilizing PCB as an effective defluoridating agent.

3.3. Optimization of sorbent dosage

The percent removal varies with different dosages of sorbent, viz., 0.1, 0.2, 0.25, 0.50, 0.75 and 1.0 g were studied to ascertain the effect of dosage and to optimize the minimum dosage required for bringing down the fluoride level to the tolerance limit. The effect of percentage removal of fluoride with different sorbent dosages is shown in Fig. 3b. The percentage removal of fluoride significantly increased with increase in sorbent dosage, which is obvious because of the increase in the number of active sites as the dosage increases [44]. The percentage of fluoride removal gradually reached a maximum and remained almost constant with the increase in dosage of sorbent. Hence, in all the subsequent experiments 0.25 g of sorbent was fixed as the optimum dosage which could give reasonably good defluoridation efficiency.

3.4. Effect of initial fluoride concentration

The effect of DC with different initial fluoride concentrations, viz., 11, 13, 15, 17 and 19 mg/L with neutral pH at 303 K were studied and are shown in Fig. 3c. The DC of PCB was found to increase with the increase in the initial concentrations of fluoride. Similar types of results were reported for fluoride removal [35,36,45].

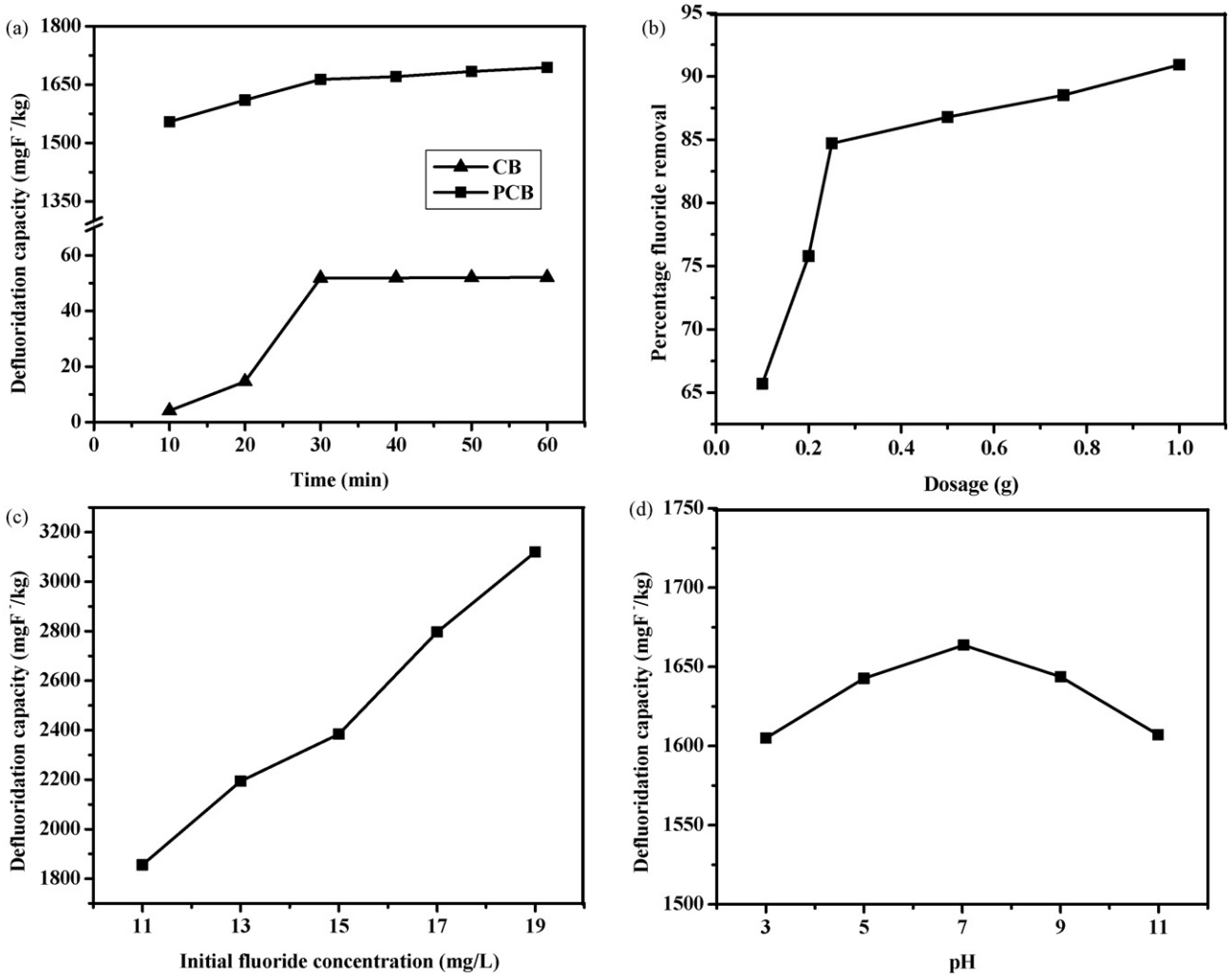

Fig. 3. Effect of (a) contact time, (b) dosage, (c) initial fluoride concentrations and (d) pH.

3.5. Influence of pH of the medium

The pH effect of the sorbent was studied at five different pH levels, viz., 3, 5, 7, 9 and 11 by keeping all other parameters constant as shown in Fig. 3d. The PCB recorded a maximum DC at pH 7 hence throughout the study pH of the medium was maintained at neutral pH. Even though there appeared to be a slight decline in DC of the sorbent in acidic as well as in alkaline medium, the differences were not significant.

3.6. Effect of competitor anions

The fluoride-contaminated drinking water contains several common other anions, viz., Cl^-, SO_4^{2-}, HCO_3^- and NO_3^- which can compete with the fluoride during sorption and hence the dependence of DC on PCB was investigated in the presence of co-anions with varying initial concentrations of these ions viz., 100, 200, 300, 400 and 500 mg/L by keeping 10 mg/L as the initial fluoride concentration with neutral pH at 303 K. The pH value of the mixed solutions of fluoride with Cl^-, SO_4^{2-}, NO_3^- and HCO_3^- were 6.78, 6.70, 6.83 and 8.23 respectively. There was a considerable increase in pH of the solution with the increase in bicarbonate concentration. Fig. 4 shows the dependence of DC on PCB in the presence of other co-anions. With the increase in the concentration of anions, a reduction in DC of PCB was observed. In the presence of other anions, there may be a competition among them for the sites on the sorbent surfaces, which is decided by the concentration, charge and size of the anions. Even though there was a decrease in DC of sorbent with an increase in the concentration of other anions, it had

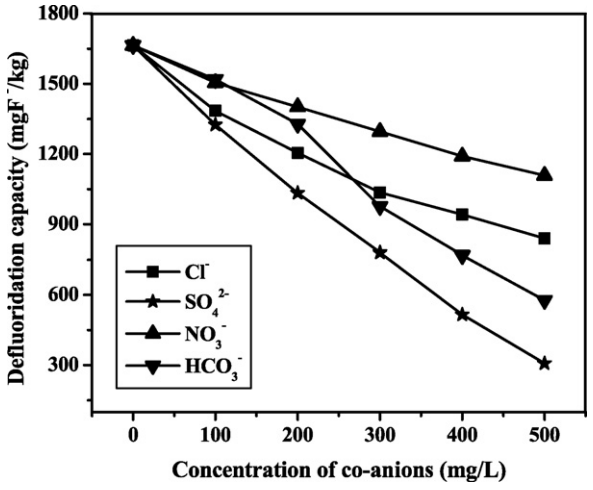

Fig. 4. Effect of coexisting anions on the DC of PCB.

Table 1
Isotherms and their linear forms

Isotherms		Linear form	Plot
Freundlich	$q_e = k_F C_e^{1/n}$	$\log q_e = \log k_F + \frac{1}{n} \log C_e$	$\log q_e$ vs. $\log C_e$
Langmuir	$q_e = \frac{Q^o b C_e}{1+bC_e}$	$\frac{C_e}{q_e} = \frac{1}{Q^o b} + \frac{C_e}{Q^o}$	$\frac{C_e}{q_e}$ vs. C_e

considerable DC and hence it could be effectively used as a defluoridating agent. This was further supported by the field trial studies of PCB.

3.7. Sorption isotherms

Freundlich and Langmuir are the two commonly used isotherms to describe the adsorption characteristics of sorbent and the linear forms of isotherms with their plots are given in Table 1.

3.7.1. Freundlich isotherm

The values of Freundlich isotherm constants, namely $1/n$ and k_F for the sorbent are listed in Table 2. The values of k_F almost remained constant in all the temperatures studied. The magnitude of the exponent $1/n$ lying between 0 and 1, and the values of n greater than 1 indicated favorable conditions for adsorption [5]. The higher correlation coefficient (r) values showed that the Freundlich isotherm fitted well with the experimental data of PCB.

3.7.2. Langmuir isotherm

The calculated values of Langmuir constants Q^o and b are listed in Table 2. The slight decrease in the values of Q^o with increasing temperature confirmed the preference of low temperature for adsorption. The correlation coefficient (r) >0.9 indicated the applicability of Langmuir isotherm for the sorption data. In order to find out the feasibility of the isotherm, the essential characteristics of the Langmuir isotherm can be expressed in terms of the dimensionless constant separation factor or equilibrium parameter [46],

$$R_L = \frac{1}{1 + bC_o} \quad (1)$$

where b is the Langmuir isotherm constant and C_o is the initial concentration of fluoride (mg/L). The R_L values at different temperatures studied were calculated and are given in Table 2. The R_L values lying between 0 and 1 indicate the favorable conditions for adsorption at all the temperatures studied [5].

3.7.3. Chi-square analysis

To identify the suitable isotherm for sorption of fluoride onto PCB, the chi-square analysis was carried out. The mathematical statement for chi-square analysis is

$$\chi^2 = \sum \frac{(q_e - q_{e,m})^2}{q_{e,m}} \quad (2)$$

where $q_{e,m}$ is equilibrium capacity obtained by calculating from the model (mg/g) and q_e is experimental data on the equilibrium capacity (mg/g). If data from the model are similar to the experimental data, χ^2 will be a small number, while if they differ, χ^2 will be a bigger number [5]. The χ^2 values for PCB was tabulated in Table 2.

Table 3
Equations of thermodynamic parameters

Thermodynamic parameters	Equations	Plot
Standard free energy change	$\Delta G^\circ = -RT \ln K_o$	$\ln \frac{q_e}{C_e}$ vs. C_e
Standard enthalpy change	$\ln K_o =$	$\ln K_o$ vs. $\frac{1}{T}$
Standard entropy change	$\frac{\Delta H^\circ}{RT} +$	
Sticking probability	$S^* = \frac{\Delta S^\circ}{R} (1-\theta) \exp\left(-\frac{E_a}{RT}\right)$	$\ln(1-\theta)$ vs. $\frac{1}{T}$

Table 4
Thermodynamic parameters for fluoride sorption onto PCB at different temperatures

Thermodynamic parameters	PCB
ΔG° (kJ mol^{-1})	
303 K	−5.06
313 K	−4.97
323 K	−4.95
ΔH° (kJ mol^{-1})	6.85
ΔS° (kJ mol^{-1} K^{-1})	5.94
E_a (kJ mol^{-1})	6.36
S^*	0.97

The χ^2 values of both isotherms did not differ much which implied that the system followed both Freundlich and Langmuir isotherms.

3.8. Thermodynamic treatment of fluoride sorption process

The feasibility of the sorption process was assessed by the thermodynamic parameters, viz., standard free energy change (ΔG°), standard enthalpy change (ΔH°), standard entropy change (ΔS°), activation energy (E_a) and sticking probability (S^*) [5,47,48] were calculated using the equations given in Table 3. The calculated values of thermodynamic parameters are shown in Table 4. The negative values of ΔG° confirmed the spontaneous nature of the sorption of fluoride onto PCB. The positive values of ΔS° which suggested F^- ions were not too restricted in the beads. The positive values of ΔH° and E_a confirmed the endothermic nature of the sorption process. The values of $S^* \sim 1$ indicated the linear sticking relationship between sorbate and sorbent due to possible mixture of physisorption and chemisorption mechanism [48].

3.9. Sorption dynamics

The two main types of sorption kinetic models, namely reaction-based and diffusion-based models, were adopted to fit the experimental data [49]. In this study, the initial sorbate concentration and the reaction temperature were considered for examining the influence of sorption capacity on the rate of the reaction.

3.9.1. Reaction-based models

To investigate the rate of the sorption of fluoride onto PCB, pseudo-first-order and pseudo-second-order kinetic models had been used at different experimental conditions. A simple pseudo-first-order kinetic model [50] is given in Table 5. Linear plots of $\log(q_e - q_t)$ against t gives a straight line that indicated the applicability of Lagergren equation. The values of k_{ad} and the correlation coefficient (r) computed from these plots for the sorbent are given

Table 2
Freundlich and Langmuir isotherm parameters of PCB

Temperature (K)	Freundlich isotherm					Langmuir isotherm				
	$1/n$	n	$k_{F\,(mg/g)}$ (L/mg)$^{1/n}$	r	χ^2	Q^o (mg/g)	b (L/g)	R_L	r	χ^2
303	0.685	1.460	1.280	0.999	0.0001	7.32	0.196	0.317	0.991	0.0002
313	0.596	1.677	1.223	0.998	0.0002	5.35	0.248	0.268	0.991	0.0003
323	0.537	1.862	1.234	0.986	0.0013	4.72	0.301	0.232	0.981	0.0015

Table 5
Kinetic models and their linear forms

Kinetic models	Linear form	Plot
Reaction-based		
Pseudo-first-order	$\log(q_e - q_t) = \log q_e - \frac{k_{ad}}{2.303} t$	$\log(q_e - q_t)$ vs. t
Pseudo-second-order	$\frac{t}{q_t} = \frac{1}{h} + \frac{t}{q_e}$	$\frac{t}{q_t}$ vs. t
Diffusion-based		
Particle diffusion	$\ln\left(1 - \frac{C_t}{C_e}\right) = -k_p t$	$\ln\left(1 - \frac{C_t}{C_e}\right)$ vs. t
Intraparticle diffusion	$q_t = k_i t^{1/2}$	q_t vs. $t^{1/2}$

Table 6
Pseudo-first-order rate constants of PCB at different temperatures with different initial concentrations

C_o (mg/L)	Mass (g)	Temperature (K)	k_{ad} (min^{-1})	r
11	0.25	303	0.204	0.997
		313	0.141	0.985
		323	0.127	0.958
13	0.25	303	0.223	0.970
		313	0.197	0.995
		323	0.126	0.991
15	0.25	303	0.238	0.972
		313	0.148	0.978
		323	0.123	0.997
17	0.25	303	0.198	0.975
		313	0.197	0.970
		323	0.140	0.949

in Table 6. The pseudo-first-order model seemed to be applicable because of the higher correlation coefficient (r).

In addition, the pseudo-second-order model was also employed to test the reaction kinetics. Although there were four types of linear pseudo-second-order kinetic models [51], the most popular linear form was used and is given in Table 5. The plot of t/q_t vs. t gives a straight line with higher correlation coefficient r values which was higher than that observed with pseudo-first-order model. This indicated the applicability of pseudo-second-order than pseudo-first-order model and the values obtained for PCB are shown in Table 7. The q_e values of the sorbent decreased with the increase in temperature, which indicated the preference of lower temperature for sorption.

The non-linear method which is applicable for the minimization of errors was also used for calculating the pseudo-second-order kinetic parameters in addition to linear method, as discussed above. As the sorbent (PCB) followed pseudo-second-order model, non-linear method was applied only to calculate pseudo-second-order kinetic parameters. In a linear analysis, different linear forms of the same model would significantly affect calculations of the parameters [52]. According to Ho [51], the non-linear method could be a better way to obtain the kinetic parameters and would make it possible to avoid such errors. For non-linear method, a trial and error procedure, which is applicable to computer operation, was developed to determine the pseudo-second-order rate parameters. An optimization routine to maximize the coefficient of determination (r^2) between experimental data and pseudo-second-order model used the solver add-in with Microsoft's spreadsheet, Microsoft Excel. In this study, the coefficient of determination, r^2, was calculated using Eq. (3) to test the best-fitting for the linear and non-linear pseudo-second-order kinetic model to the experimental data,

$$r^2 = \sum \frac{(q_m - \bar{q}_t)^2}{(q_m - \bar{q}_t)^2 + (q_m - q_t)^2} \quad (3)$$

where q_m is the amount of fluoride on the surface of the bead at any time, t (mg/g) obtained from the second-order kinetic model, q_t is the amount of fluoride on the surface of the bead at any time, t (mg/g) obtained from experiment and $\bar{q}_t$ is the average of q_t (mg/g). The coefficient of determination (r^2) calculated for both the linear and non-linear methods of pseudo-second-order model for PCB is presented in Table 7 with q_e, k and h values. Higher r^2 values of non-linear method indicated a better applicability of non-linear pseudo-second-order method than the linear one.

3.9.2. Diffusion-based models

For a solid–liquid sorption process, the solute transfer is usually characterized either by particle diffusion [5,53] or by intraparticle diffusion [54] control. The equations for both the diffusion models are given in Table 5. The values of k_p, k_i and r are presented in

Table 7
Comparison of the linear and non-linear methods of pseudo-second-order kinetic parameters of PCB based on coefficient of determination (r^2)

Methods	Parameters	303 K				313 K				323 K			
		11 mg/L	13 mg/L	15 mg/L	17 mg/L	11 mg/L	13 mg/L	15 mg/L	17 mg/L	11 mg/L	13 mg/L	15 mg/L	17 mg/L
Linear	q_e (mg/g)	2.183	2.520	2.913	3.369	1.996	2.237	2.512	2.795	1.925	2.152	2.458	2.736
	k (g/mg min)	0.101	0.094	0.071	0.054	0.169	0.241	0.272	0.228	0.206	0.313	0.311	0.230
	h (mg/g min)	0.482	0.594	0.604	0.618	0.672	1.205	1.715	1.785	0.762	1.449	1.876	1.722
	r	0.997	0.997	0.998	0.994	0.999	0.999	1.00	1.00	1.00	0.999	1.00	0.999
	r^2	0.635	0.640	0.635	0.620	0.697	0.695	0.726	0.740	0.748	0.761	0.781	0.718
Non-linear	q_e (mg/g)	1.871	2.151	2.457	2.758	1.837	2.071	2.381	2.646	1.781	2.049	2.363	2.572
	k (g/mg min)	0.090	0.084	0.063	0.038	0.163	0.236	0.269	0.225	0.201	0.310	0.309	0.227
	h (mg/g min)	0.315	0.389	0.380	0.289	0.550	1.012	1.525	1.575	0.638	1.302	1.725	1.502
	r^2	0.998	0.996	0.999	0.998	0.993	0.987	0.997	0.995	0.988	0.993	0.998	0.991

Table 8
Particle and intraparticle diffusion model parameters for fluoride sorption on PCB at different initial concentrations with different temperatures

C_o (mg/L)	Mass (g)	303 K				313 K				323 K			
		Particle DM[a]		Intraparticle DM[a]		Particle DM[a]		Intraparticle DM[a]		Particle DM[a]		Intraparticle DM[a]	
		k_p (min^{-1})	r	k_i (mg/g min $^{0.5}$)	r	k_p (min^{-1})	r	k_i (mg/g min$^{0.5}$)	r	k_p (min^{-1})	r	k_i (mg/g min $^{0.5}$)	r
11	0.25	0.063	0.923	0.351	0.960	0.045	0.920	0.328	0.942	0.038	0.933	0.316	0.931
13	0.25	0.077	0.932	0.407	0.956	0.046	0.883	0.373	0.917	0.035	0.903	0.357	0.902
15	0.25	0.104	0.982	0.463	0.966	0.050	0.867	0.420	0.904	0.042	0.945	0.406	0.892
17	0.25	0.151	0.956	0.533	0.965	0.058	0.983	0.457	0.897	0.046	0.814	0.459	0.908

[a] DM: diffusion model.

Table 9
SSE values of kinetic models employed for sorption of fluoride onto PCB

Kinetic models	303 K				313 K				323 K			
	11 mg/L	13 mg/L	15 mg/L	17 mg/L	11 mg/L	13 mg/L	15 mg/L	17 mg/L	11 mg/L	13 mg/L	15 mg/L	17 mg/L
Pseudo-first-order	0.0007	0.0013	0.0037	0.0011	0.0040	0.0013	0.0094	0.0016	0.0082	0.0170	0.0200	0.0110
Pseudo-second-order	0.0005	0.0010	0.0023	0.0008	0.0013	0.0010	0.0032	0.0012	0.0065	0.0024	0.0016	0.0039
Particle diffusion	0.3830	0.3220	0.2670	0.2110	0.4290	0.3540	0.3140	0.2670	0.4690	0.4220	0.3600	0.3210
Intraparticle diffusion	0.0190	0.0210	0.0180	0.0130	0.0350	0.0520	0.0610	0.0680	0.0440	0.0630	0.0700	0.0560

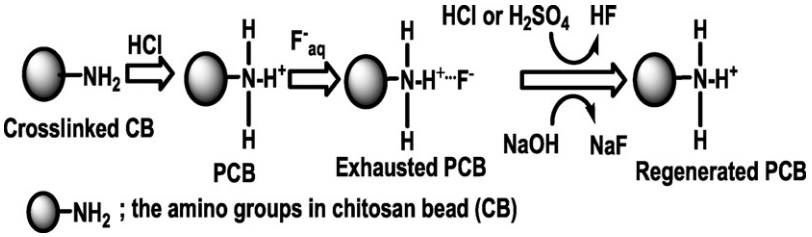

Scheme 1. Mechanism of fluoride sorption on PCB and its regeneration.

Table 8, and the higher r values in both the cases indicated the possibility of sorption process being controlled by both the particle and intraparticle diffusion models.

3.9.3. Fitness of the kinetic models

The best-fit among the kinetic models was assessed by the squared sum of errors (SSE) values. It is assumed that the model which gives the lowest SSE values is the best model for the particular system [5,49]. The SSE values were calculated by the equation,

$$\mathrm{SSE} = \sum \frac{(q_{t,e} - q_{t,m})^2}{q_{t,e}^2} \quad (4)$$

where $q_{t,e}$ and $q_{t,m}$ are the experimental sorption capacity of fluoride (mg/g) at time t and the corresponding value that is obtained from the kinetic models. SSE values for all the kinetic models were calculated and are summarized in Table 9. It was once again confirmed that pseudo-second-order model which had lower SSE values seemed to be best reaction-based model than the pseudo-first-order model. Among the diffusion-based models, the intraparticle diffusion model was found to have lower SSE values which indicated that the sorbent removed fluoride by intraparticle diffusion rather than particle diffusion.

3.10. Sorption mechanism

A slight widening of $-NH_2$ stretching band in FTIR spectra of the fluoride treated PCB (cf. Fig. 1c) confirmed the presence of hydrogen bonding between protonated amine (NH_3^+) and fluoride suggesting that the PCB removed fluoride by means of hydrogen bonding which is an electrostatic adsorption between positively charged surface and negatively charged fluoride ions. The mechanism of fluoride removal by PCB is shown in Scheme 1. Moreover, PCB may be considered as hard acid as they possess H^+ ion and hence would prefer to bind with hard base, most preferably with high electronegative and low polarisable F^- ion [55].

3.11. Fluoride desorption

The exhausted PCB was regenerated with eluents like HCl, H_2SO_4 and NaOH. All the regeneration experiments were carried out at room temperature. Mineral acids elute fluoride from exhausted PCB as HF and NaOH as NaF (cf. Scheme 1). Desorption efficiency of PCB was studied using 0.1 M HCl, 0.1 M H_2SO_4 and 0.1 M NaOH as eluents. Out of the three eluents, HCl had been identified as the best eluent as it has 94.5% desorption efficiency whereas H_2SO_4 has 89% and NaOH showed a maximum of 85% desorption efficiency.

Table 10
Field trial results of PCB

Water quality parameters	Before treatment	After treatment
F^- (mg/L)	2.33	0.90
pH	9.10	6.21
Electrical conductivity (ms/cm)	0.87	0.65
Cl^- (mg/L)	56.80	42.60
Total hardness (mg/L)	70.00	0.00
Total dissolved solids (mg/L)	473.00	465.00
Na^+ (mg/L)	55.10	51.60
K^+ (mg/L)	8.80	5.90

3.12. Field studies

The applicability of PCB in the field condition was tested with water samples taken from a nearby fluoride endemic area and the results are listed in Table 10. The sorbent reduced the level of fluoride concentration from 2.33 mg/L to the desired level using 0.5 g of PCB for 50 ml of sample, and the time of contact was fixed at 30 min at room temperature. To some extent PCB also removed other ions present in water in addition to fluoride. Even though the sorbent was influenced by the presence of foreign anions, this factor did not affect lowering the fluoride level to the tolerance limit in field conditions.

4. Conclusions

PCB possessed higher DC than the raw chitosan bead. The DC of PCB was independent of pH and altered in presence of co-existing anions. The adsorption pattern followed both Freundlich and Langmuir isotherms. The values of thermodynamic parameters confirmed the spontaneous and endothermic nature of the fluoride sorption. The rate of reaction of the sorbent followed pseudo-second-order kinetics and non-linear pseudo-second-order model would be a better way to obtain kinetic parameters. The sorption of fluoride onto PCB followed intraparticle diffusion pattern. Field trial results indicated that PCB could be employed as a

best sorbent for fluoride removal. The PCB is an effective, inexpensive and replicable material which could be employed for defluoridation and it removes fluoride by adsorption mechanism.

Acknowledgements

The authors are thankful to University Grants Commission (No. F.30-56/2004(SR)), New Delhi, India for the provision of financial support to carry out this research work.

References

[1] Y. Veressinina, M. Trapido, V. Ahelik, R. Munter, Fluoride in drinking water: the problem and its possible solutions, Proc. Estonian Acad. Sci. Chem. 50 (2001) 81–88.
[2] K. Sarala, P.R. Rao, Endemic fluorosis in the Village Ralla, Anantapuram in Andhra Pradesh—an epidemiological study, Fluoride 26 (1993) 177–180.
[3] WHO Report, Fluoride and Fluorides: Environmental Health Criteria, World Health Organisation, 1984.
[4] S. Meenakshi, Ph.D Thesis, Studies on Defluoridation of Water with a Few Adsorbents and Development of an Indigenous Defluoridation Unit for Domestic Use, Gandhigram, Tamil Nadu, India, 1992.
[5] S. Meeenakshi, N. Viswanathan, Identification of selective ion exchange resin for fluoride sorption, J. Colloid Interface Sci. 308 (2007) 438–450.
[6] N. Parthasarathy, J. Buffle, W. Haerdi, Study of interaction of polymeric aluminium hydroxide with fluoride, Can. J. Chem. 64 (1986) 24–29.
[7] K.M. Popat, P.S. Anand, B.D. Dasare, Selective removal of fluoride ions from water by the aluminium form of the aminomethylphosphonic acid-type ion exchanger, React. Polym. 23 (1994) 23–32.
[8] S.V. Joshi, S.H. Mehta, A.P. Rao, A.V. Rao, Estimation of sodium fluoride using HPLC in reverse osmosis experiments, Water Treat. 7 (1992) 207–211.
[9] R. Simons, Trace element removal from ash dam waters by nanofiltration and diffusion dialysis, Desalination 89 (1993) 325–341.
[10] S.K. Adhikary, U.K. Tipnis, W.P. Harkare, K.P. Govindan, Defluoridation during desalination of brackish water by electro dialysis, Desalination 71 (1989) 301–312.
[11] M. Hichour, F. Persin, J. Sandeaux, C. Gavach, Fluoride removal from waters by Donnan dialysis, Sep. Purif. Technol. 18 (2000) 1–11.
[12] S. Kagne, S. Jagtap, P. Dhawade, S.P. Kamble, S. Devotta, S.S. Rayalu, Hydrated cement: a promising adsorbent for the removal of fluoride from aqueous solution, J. Hazard. Mater. 154 (2008) 88–95.
[13] C. Sairam Sundaram, N. Viswanathan, S. Meenakshi, Defluoridation chemistry of synthetic hydroxyapatite at nano scale: equilibrium and kinetic studies, J. Hazard. Mater. 155 (2008) 206–215.
[14] A.A.M. Daifullah, S.M. Yakout, S.A. Elreefy, Adsorption of fluoride in aqueous solutions using $KMnO_4$-modified activated carbon derived from steam pyrolysis of rice straw, J. Hazard. Mater. 147 (2007) 633–643.
[15] D. Mohan, K.P. Singh, V.K. Singh, Wastewater treatment using low cost activated carbons derived from agricultural byproducts—a case study, J. Hazard. Mater. 152 (2008) 1045–1053.
[16] M. Islam, R.K. Patel, Evaluation of removal efficiency of fluoride from aqueous solution using quick lime, J. Hazard. Mater. 143 (2007) 303–310.
[17] H. Wang, J. Chen, Y. Cai, J. Ji, L. Liu, H.H. Teng, Defluoridation of drinking water by Mg/Al hydrotalcite-like compounds and their calcined products, Appl. Clay Sci. 35 (2007) 59–66.
[18] S. Meenakshi, C. Sairam Sundaram, R. Sukumar, Enhanced fluoride sorption by mechanochemically activated kaolinites, J. Hazard. Mater. 153 (2008) 164–172.
[19] A. Tor, Removal of fluoride from an aqueous solution by using montmorillonite, Desalination 201 (2006) 267–276.
[20] N.I. Chubar, V.F. Samanidou, V.S. Kouts, G.G. Gallios, V.A. Kanibolotsky, V.V. Strelko, I.Z. Zhuravlev, Adsorption of fluoride, chloride, bromide, and bromate ions on a novel ion exchanger, J. Colloid Interface Sci. 291 (2005) 67–74.
[21] Y. Zhao, X. Li, L. Liu, F. Chen, Fluoride removal by Fe(III)-loaded ligand exchange cotton cellulose adsorbent from drinking water, Carbohydr. Polym. 72 (2008) 144–150.
[22] W. Nigussie, F. Zewge, B.S. Chandravanshi, Removal of excess fluoride from water using waste residue from alum manufacturing process, J. Hazard. Mater. 147 (2007) 954–963.
[23] M.G. Sujana, H.K. Pradhan, S. Anand, Studies on sorption of some geomaterials for fluoride removal from aqueous solutions, J. Hazard. Mater. 161 (2009) 120–125.
[24] V. Gopal, K.P. Elango, Equilibrium, kinetic and thermodynamic studies of adsorption of fluoride onto plaster of Paris, J. Hazard. Mater. 141 (2007) 98–105.
[25] A.K. Yadav, C.P. Kaushik, A.K. Haritash, A. Kansal, N. Rani, Defluoridation of groundwater using brick powder as an adsorbent, J. Hazard. Mater. 128 (2006) 289–293.
[26] A. Eskandarpour, M.S. Onyango, A. Ochieng, S. Asai, Removal of fluoride ions from aqueous solution at low pH using schwertmannite, J. Hazard. Mater. 152 (2008) 571–579.
[27] C. Sairam Sundaram, N. Viswanathan, S. Meenakshi, Uptake of fluoride by nano-hydroxyapatite/chitosan, a bioinorganic composite, Bioresour. Technol. 99 (2008) 8226–8230.
[28] H.K. An, B.Y. Park, D.S. Kim, Crab shell for the removal of heavy metals from aqueous solution, Water Res. 35 (2001) 3551–3556.
[29] R.A.A. Muzzarelli, Natural Chelating Polymers: Alginic acid Chitin and Chitosan, Pergamon Press, New York, 1973.
[30] L. Jin, R. Bai, Mechanisms of lead adsorption on chitosan/PVA hydrogel beads, Langmuir 18 (2002) 9765–9770.
[31] S.P. Kamble, S. Jagtap, N.K. Labhsetwar, D. Thakare, S. Godfrey, S. Devotta, S.S. Rayalu, Defluoridation of drinking water using chitin, chitosan and lanthanum-modified chitosan, Chem. Eng. J. 129 (2007) 173–180.
[32] K. Jaafari, S. Elmaleh, J. Coma, K. Benkhouja, Equilibrium and kinetics of nitrate removal by protonated cross-linked chitosan, Water SA 27 (2001) 9–13.
[33] W. Ma, F.Q. Ya, M. Han, R. Wang, Characteristics of equilibrium, kinetics studies for adsorption of fluoride on magnetic-chitosan particle, J. Hazard. Mater. 143 (2007) 296–302.
[34] E. Guibal, C. Milot, J.M. Tobin, Metal-anion sorption by chitosan beads: equilibrium and kinetic studies, Ind. Eng. Chem. Res. 37 (1998) 1454–1463.
[35] N. Viswanathan, S. Meenakshi, Selective sorption of fluoride using Fe (III) loaded carboxylated chitosan beads, J. Fluorine Chem. doi:10.1016/j.jfluchem.2008.03.005.
[36] N. Viswanathan, S. Meenakshi, Enhanced fluoride sorption using La (III) incorporated carboxylated chitosan beads, J. Colloid Interface Sci. 322 (2008) 375–383.
[37] APHA, Standard Methods for the Examination of Water and Waste Water, American Public Health Association, Washington, DC, 2005.
[38] M.V. Lopez-Ramon, F. Stoeckli, C. Moreno-Castilla, F. Carrasco-Marin, On the characterization of acidic and basic surface sites on carbons by various techniques, Carbon 37 (1999) 1215–1221.
[39] N. Li, R. Bai, A novel amine-shielded surface cross-linking of chitosan hydrogel beads for enhanced metal adsorption performance, Ind. Eng. Chem. Res. 44 (2005) 6692–6700.
[40] L.G. Wade, Organic Chemistry, 4th ed., Prentice Hall, New Jersey, 1999.
[41] H.S. Nalwa, Conductive Polymers: Spectroscopy and Physical Properties Handbook of Organic Conductive Molecules and Polymers, vol. 3, John Wiley & Sons Ltd., Chichester, 1997.
[42] B. Smith, Infrared Spectral Interpretation—A Systematic Approach, CRC Press, London, 1998.
[43] Y.S. Al-Degs, M.I. El-Barghouthi, A.A. Issa, M.A. Khraisheh, G.M. Walker, Sorption of Zn (II), Pb (II) and Co (II) using natural sorbents: equilibrium and kinetic studies, Water Res. 40 (2006) 2645–2658.
[44] A. Mellah, S. Chegrouche, The removal of zinc from aqueous solutions by natural bentonite, Water Res. 31 (1997) 621–629.
[45] L. Lv, J. He, M. Wei, D.G. Evans, Z. Zhou, Treatment of high fluoride concentration water by $MgAl\text{-}CO_3$ layered double hydroxides: kinetic and equilibrium studies, Water Res. 41 (2007) 1534–1542.
[46] T.W. Weber, R.K. Chakravorti, Pore and solid diffusion models for fixed bed adsorbers, J. Am. Inst. Chem. Eng. 20 (1974) 228–238.
[47] A.A. Khan, R.P. Singh, Adsorption thermodynamics of carbofuran on Sn (IV) arsenosilicate in H^+, Na^+ and Ca^{2+} forms, Colloids Surf. 24 (1987) 33–42.
[48] M. Horsfall, A.I. Spiff, Effects of temperature on the sorption of Pb^{2+} and Cd^{2+} from aqueous solution by caladium bicolor (wild cocoyam) biomass, Electron. J. Biotechnol. 8 (2005) 162–169.
[49] Y.S. Ho, J.C.Y. Ng, G. McKay, Kinetics of pollutant sorption by biosorbents: review, Sep. Purif. Methods 29 (2000) 189–232.
[50] S. Lagergren, Zur theorie der sogenannten adsorption gelöster stoffe, K. Sven. Vetenskapsakad. Handl. 24 (1898) 1–39.
[51] Y.S. Ho, Second order kinetic model for the sorption of cadmium onto tree fern: a comparison of linear and non linear methods, Water Res. 40 (2006) 119–125.
[52] D.G. Kinniburgh, General purpose adsorption isotherms, Environ. Sci. Technol. 20 (1986) 895–904.
[53] M. Chanda, K.F. O'Driscoll, G.L. Rempel, Sorption of phenolics onto cross-linked poly (4-vinyl pyridine), React. Polym. 1 (1983) 281–293.
[54] W.J. Weber, J.C. Morris, Equilibria and capacities for adsorption on carbon, J. Sanitary Eng. Div. 90 (1964) 79–91.
[55] R.G. Pearson, Hard and soft acids and bases, J. Am. Chem. Soc. 85 (1963) 3533–3539.